17th International Conference on Environmental Science and Technology

Athens, Greece, 1 to 4 September 2021

Functionalized iron oxide nanocomposite ultrafiltration membranes for water-in-oil emulsion separation

Wadi V.S.[1], Ouda M.[1], Naddeo V.[2], Banat F.[1], and Hasan S.W.[1*]

[1]Center for Membranes and Advanced Water Technology (CMAT), Department of Chemical Engineering, Khalifa University of Science and Technology, P.O. Box 127788, Abu Dhabi, United Arab Emirates

[2]Sanitary Environmental Engineering Division (SEED), Department of Civil Engineering, University of Salerno - Via Giovanni Paolo II #132, 84084 Fisciano (SA), Italy

*corresponding author:
e-mail: shadi.hasan@ku.ac.ae

Abstract. Removal of emulsified water in oil (w/o) emulsions are the most challenging compared to free water and dissolved water emulsions. Emulsified w/o cannot be removed by conventional techniques such as settling tanks, oil skimmers, floatation and magnetic technologies. Membrane technology is a highly efficient, energy saving, and pollutant free alternative. In this work, iron oxide-oleylamine nanoparticles have been synthesized and embedded into polylactic acid (PLA) to make a hydrophobic-super-oleophilic ultrafiltration membrane. The concentration of the nanoparticles was varied from 0.5 to 3% of the polymer. Scanning electron microscopy (SEM), Energy dispersive X-ray spectroscopy (EDS), thermal gravimetric analysis (TGA), and Fourier-transform infrared radiation (FTIR) were utilized to confirm both the attachment of the oleylamine on the iron oxide and the loading of the prepared nanoparticles into the PLA membrane. The water contact angle was found to increase steadily as the concentration of the nanocomposites increased. This was associated with the hydrophobicity of the membranes, allowing the oil to penetrate through the membrane. Moisture removal in surfactant-stabilized w/o emulsions reached up to 80% in the composite membranes, compared to only 52% in the pristine PLA. The maximum permeability was found to be at 2% loading, where 885 L/m^2.h/bar was reported, compared to 500 L/m^2.h/bar in the PLA. The abundance of iron-oxide, and the biodegradability of PLA prove the capability of the prepared membranes to be a viable and environmentally friendly alternative for w/o separation.

Keywords: Super-hydrophobic; water in oil; iron oxide; ultrafiltration; chemical synthesis.

1. Introduction

The limitation of freshwater resources globally has driven dependence on other methods of potable water production, such as desalination [1]. Membrane distillation (MD) is an emerging method of desalination, in which the temperature difference across a porous membrane drives the water purification process [2]. Membrane features such as hydrophobicity, thermal and chemical stability, and porosity will determine the performance of the membrane in this application [3, 4]. A higher hydrophobicity of the membrane material is expected to enhance the flux and removal of the MD process due to lower surface wettability [5]. Incorporation of nanomaterials into polymeric membranes is a common method of achieving this property [6, 7]. Iron oxide is an abundant and cost-effective metal oxide that has multiple properties [8, 9]. However, its hydrophilicity can limit its efficiency in membrane distillation. Another important challenge in membrane filtration is the reusability and recyclability of the used membranes, disposal of synthetic membrane may cause addition pollution in the environment. Thus, in this current work we report on the development of environmentally friendly, biodegradable PLA composites membranes embedded with the functionalized Fe_2O_3 for oil/water emulsion removal. The addition of hydrophobic iron nanoparticles improves the overall hydrophobicity of the member which can effetely used to removal of oil from in oil/water emulsion.

Materials and methods

Functionalized Fe_2O_3 – oleylamine (Fe-OL) was prepared according to Tzitzios et al [10]**,** Initially 1.5g of $FeCl_3.6H_2O$ in 20 ml of oleylamine was mixed and contineously stirrered at 80 °C via a magnetic stirrer until a transparent solution starts to form. The temperature was then raised to 250°C, and this temperature was maintained for at least 1 hr. After it was left to cool down to room temperature, a sufficient volume of ethanol was used to precipitate the resultant solution. To obtain the nanoparticles, the solution was then centrifuged for 20 mins. The Fe-Ol powder was then dried at 60 ºC overnight to get a powdered product. Hydrophilic Fe-OH nanoparticles were also prepared by co precipataion for comparision and characterized. via Thermal gravimetric analysis (TGA), Fourier transform infrared spectrometry (FTIR), Scanning electron microscopy (SEM), particle size, and X-ray diffraction (XRD).

Fabrication of pristine PLA and PLA-Fe-OL composite membranes

The membranes in this work were prepared by non-solvent induced phase separation (NIPS) method using dope solutions containing PLA, PVP, and different Fe-OL filler loading. The amount of PLA, PVP and Fe-OL used are listed in Table **1**.

Table 1. Concentration of dope solutions used for nanocomposite membrane fabrication

Label	Mass of PLA (g)	Mass of PVP (g)	Fe-OL (wt.%)*	Total mass (g)
PLA	2.4	0.3	0	15
M1	2.4	0.3	0.5	15
M2	2.4	0.3	1.0	15
M3	2.4	0.3	1.5	15
M4	2.4	0.3	2.0	15
M5	2.4	0.3	3.0	15

*The percentage of nanomaterial is with respect to the total weight of the PLA used.

2. Results and Discussion

Super hydrophobic iron (Fe_2O_3) nanoparticles were prepared by thermolytic decomposition of $FeCl_3$. 6 H_2O at high temperature using oleylamine as solvent as well as capping agent. **Figure 1a** shows the schematic representation of iron nanoparticle covered with the oleylamine molecules.

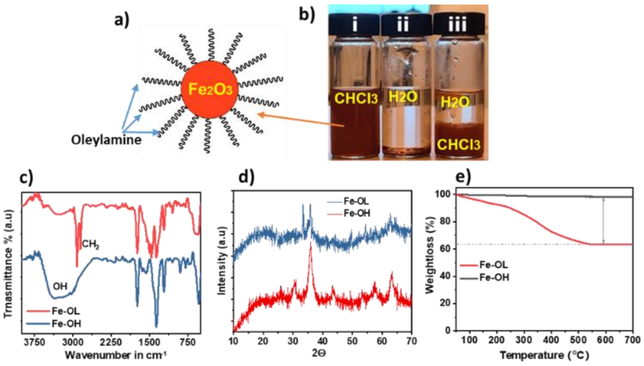

Figure 1. TGA analysis of pristine and modified MWCNT.

The long alkyl chains on the surface of iron nanoparticles impart high hydrophobic property and also helps in improve the dispersion in the organic solvents. **Figure 1b** clearly shows that the Fe-OL nanoparticles are homogeneously dispersed and are highly stabile and in chloroform, whereas, in water the nanoparticles were agglomerated and settled in the bottom of the vial further supports the superior organophilic nature of the nanoparticles. The hydrophobic alkyl chains on the surface strongly repel the water, however improve the interaction with the organic solvents or oils, thus, can be effectively used in removal of suspended oils from the industrial wastewater. The successful formation of the oleylamine caped iron nanoparticles was confirmed by the FTIR spectroscopy. The hydrophilic Fe_2O_3 (Fe-OH) was also prepared by coprecipitation techniques for comparison. In **Figure 1c**, peaks observed at 698, 638 and 580 cm^{-1} in both the Fe-OL and Fe-OH are assigned for the Fe-O bond. The broad peak around 3300 cm^{-1} in Fe-OH are due to the presence of surface hydrophilic OH groups. however, in Fe-OL spectra this peak intensity is reduced and shifted to 3230 cm^{-1} due to the attachment of amine group from oleylamine, moreover, two new prominent peaks appeared at 2923 cm^{-1} and 2862 cm^{-1} are due to -CH and -CH_3 stretching vibration from alkyl chain further confirms the presence of oleylamine on the iron nanoparticles. The X-ray diffractogram (XRD in **Figure 1d**) of Fe-OL and Fe-OH displayed the diffraction peaks at 2θ equal to 30.1°, 35.4°, 43.1°, 53.4°, 57.1°, and 62.6° which are indexed as (220), (311), (400), (511), and (440) lattice, respectively are in good agreement with structure of maghemite (JCPDS 19-629) suggest the formation of iron nanoparticles by both coprecipitation and thermal decomposition method. Thermogravimetric analysis (TGA) was used to determine the presence of oleylamine on iron particles. **Figure 1e** presents the weight loss comparison between of Fe-OH and oleylamine capped Fe-OL. The thermogram indicate that the Fe-OH is stable up to 700 °C and did not showed any weight loss suggests the high stability of the nanoparticles, however, Fe-OL displayed two step broad weight loss between 100 °C to 500 °C, in first step the weight loss between 100 to 200 °C could be due to the presence of trace amount of unattached free oleyl amine [11]. The second step initiated around 200 °C showed gradual weight loss till 500 °C, the higher decomposition temperature compared to pure oleylamine also indicate strong interaction between oleylamine and iron nanoparticles. The weight loss between 250 to 500 °C indicate the amount of oleyleamine present on the iron nanoparticles and was found approximately 32 wt% to the total weight.

PLA hybrid membranes were prepared by adding different amount of Fe-OL. **Table 1** displays the properties of the fabricated nanocomposite membranes. The contact water angle of the composite membranes is found to increase with increasing filler concentration. This is expected due to the high hydrophobicity of the material, and as a result of the 18-carbon chain in the oleylamine. However, at the highest concentrations, there is a sharp decline. This can be due to the formation of defects and a non-homogenous membrane formed due to the high nanocomposite loading. The hydrophobicity of the material limits its complete dissolution in the dope solution.

Table 2. Contact angle, porosity, and liquid entry pressure of nanocomposite membranes.

Membrane	**Contact angle (°)**	**Porosity (%)**	**Pore size**
PLA	75.86±1.9	43.3±0.45	84.3±0.1
M-1	80.62±1.1	45.66±0.53	87.34±0.1
M-2	82.73±1.8	44.7±0.51	96.11±0.7
M-3	81.6±0.9	44.86±0.6	100.66±1.4
M-4	88.2±1.04	37.26±0.89	126.84±2.0
M-5	89.1±0.4	35.40±0.91	103.87±1.6

The pore size of pure PLA was around 43%, with the addition of 0.5 wt% of Fe-OL the pore size increased to 45.6 and aging showed decrease trend, at 2.5 and 3.0 wt% of Fe-OL loading the porosity decreased to 37 and 35 % respectively. Reduced porosity could be due to the increased hydrophobicity of the membrane by the addition of Fe-OL which slowdown the dissolution of PVA, this also leads to increase in pore size as observed in **Table 1**.

FT-IR and TGA of the nanohybride membranes were used to further confirm the presence and interaction of Fe-OL nanomaterials with PLA chains. **Figure 2** shows the FT-IR, TGA and DTG spectra of the pure PLA and their corresponding nanohybrid membranes. The PLA FT-IR spectrum shows characteristic stretching frequencies for C=O, $–CH_3$ asymmetric, $–CH_3$ symmetric, and C–O, at 1746, 2995, 2946 and 1080 cm^{-1}, respectively [12]. Bending frequencies for $–CH_3$ asymmetric and –CH3 symmetric have been identified at 1452 and 1361 cm^{-1}, respectively. Similar peaks were also observed in nanohybrids membranes, the Fe-OL peaks in the nanohybrid are not well distinguishable due to the low concentration and also due to the overlapping of Fe-OL peaks with the PLA peaks, however, a slight increase in the peak intensity around 2995 to 2800 cm^{-1} was observed with the increase in the Fe-OL content which is attributed to the alkyl chains peaks in oleylamine.

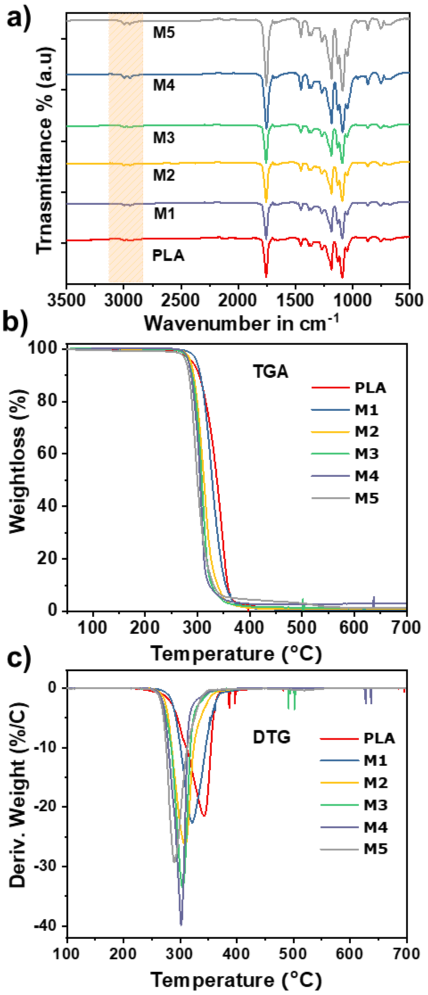

Figure 2 a) FTIR, b) TGA and c) DTG curve for the PLA and PLA-Fe-OL nanohybrid membranes

The TGA and DTG curves obtained for all the fabricated membranes are shown in **Figure 2** (**b** and **c**) respectively. The pristine PLA and nanohybrid membranes display a single degradation step, the initial degradation step in PLA initiates at 295 ºC, however, this temperature staidly decreased with the increase in the Fe-OL content in the nanohybrid membranes. For instance, M1 with the lowest Fe-OL loading (0.5 wt%) the initial degradation starts around 293 ºC, whereas, with the increase in Fe-OL loading from 2, 2.5 and 3 wt% in M3, M4 and M5 respectively, the initial degradation temperature decreased to 285 ºC, 283 ºC and 276 ºC respectively. Moreover, the final degradation temperature also decreased with respect to their corresponding nanomaterial loading. Furthermore, the nanohybrid membranes displayed higher residues at 700 ºC corresponding to their initial iron nanoparticles loading. The decrease in the initial degradation with filler loading was also supported by the DTG curve (see **Figure 2c**). This could be due to the presence of oleylamine chains on the surface of iron nanoparticles, these free moving alkyl chains can act as plasticizers with in the PLA matrix causing higher chain mobility, thus increasing temperature results in faster degradation of nanohybrids. However, it should be noted that the degradation temperature is within the operating limit and hence, the small difference in the degradation temperature does not impact on the performance of the membrane.

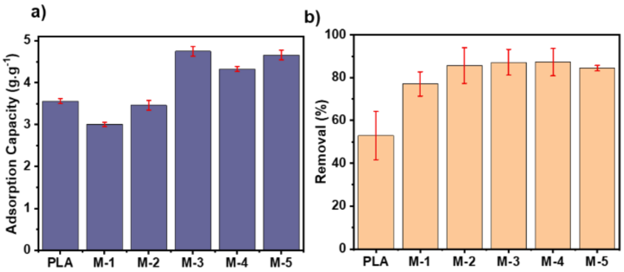

Figure 3. a) Oil adsorption, b): oil removal of PLA and their respective hybrid membranes.

To study the effect of the Fe-OL in PLA nanohybrid membranes oil adsorption, a pknow weigh of films was dipped in to the oil/water emussion then studied its oil adsorption capacity by measuring weight difference before and after immersion. **Figure 3a** shows increasing in oil adsorption with the increasing the Fe-OL nanoparticles. However, the adsorption is not very much high compared to the pure PLA, this could be due to the adsorption taking place only at the surface of the membrane.

The oil/water emulsion in this study was prepared by mixing oil with water in the volume ratio of 1:100 in presence of SDS surfactant followed by ultrasonic treatment for 1.5 h at the temperature of 25 °C ~ 30 °C to obtain the milky emulsion. The emulsion stabilized at least 4 h before use. A dead-end glass filter with a stainless-steel support base (ϕ 47 mm, LukeGL) was used to evaluate the emulsion separation performance of the membranes. The separatation of oil from the oil/water emlussion is shown in **Figure 3b**, it is clearly seen that PLA nanohybrid membranes showed higher removal capacity than the pristine PLA membranes, Pristine PLA showed around 50 % separation, where as addition of 0.5 wt% Fe-OL significantly improved the removal to 76%, moreover, with the increasing the nanomaterial increased the removal efficiency and maximum of 83% was achieved for M3 with 2.0 wt% of Fe-OL. Further increase in the nanomaterials decreased the separation efficiency could be due to the agglomeration of the nanoparticles inside the membranes.

Thus, it can be concluded that the addition of super hydrophobic nanomaterials could significantly enhance the oil/water separation capacity of the PLA membrane.

Conclusion

Oleylamine functionalized super hydrophobic Fe_2O_3, nanomaterials were prepared using oleylamine as solvent and capping agent. The nonpolar long chain hydrocarbon formed a ring outside the Fe_2O_3 molecule resulted in enhanced hydrophobicity that can be made suitable to separate organophilic solvents/emulsions. The super hydrophobic Fe-OL nanoparticles were well characterized and are used as filler in PLA membranes to enhance the hydrophobic character of the PLA. Varying amounts of Fe-OL were used to prepare different composition PLA nanohybrid membranes. The nanohybrid membranes showed uniform dispersion of Fe-OL nanoparticles due to the compatibility of oleylamine chains with the PLA alkyl chain. The porosity of the membranes showed increased trend up to 2.5 wt% Fe-OL loading, further increase in the loading decreased the porosity. The contact angle of the membranes much improved by the addition of Fe-OL and reached 89 ^{o}C with 2.5 wt% addition compared to 75 in pure PLA. The addition of 0.5 wt% of Fe-OL significantly improved the oil separation ability from the oil/water emulsion. Highest separation of 83% was achieved with only 2.0 wt% loading nanoparticles. The separation efficiency improved with the addition of super hydrophobic nanoparticles which can also applied for other membranes. Easy preparation of Fe-OL, bio compatibility and degradability of PLA add an advantage in reducing environmental pollution by membranes. can effectively use in oil separation from oil/water emulsion.

References

[1] S. Jamaly, N.N. Darwish, I. Ahmed, S.W. Hasan, A short review on reverse osmosis pretreatment technologies, Desalination 354 (2014) 30-38.

[2] J. Zuo, S. Bonyadi, T.-S. Chung, Exploring the potential of commercial polyethylene membranes for desalination by membrane distillation, Journal of Membrane Science 497 (2016) 239-247.

[3] D. Hou, H. Fan, Q. Jiang, J. Wang, X. Zhang, Preparation and characterization of PVDF flat-sheet membranes for direct contact membrane distillation, Separation and Purification Technology 135 (2014) 211-222.

[4] M. Gryta, M. Barancewicz, Influence of morphology of PVDF capillary membranes on the performance of direct contact membrane distillation, Journal of Membrane Science 358(1) (2010) 158-167.

[5] A.C.M. Franken, J.A.M. Nolten, M.H.V. Mulder, D. Bargeman, C.A. Smolders, Wetting criteria for the applicability of membrane distillation, Journal of Membrane Science 33(3) (1987) 315-328.

[6] K.-J. Lu, J. Zuo, T.-S. Chung, Tri-bore PVDF hollow fibers with a super-hydrophobic coating for membrane distillation, Journal of Membrane Science 514 (2016) 165-175.

[7] F. Ardeshiri, S. Salehi, M. Peyravi, M. Jahanshahi, A. Amiri, A.S. Rad, PVDF membrane assisted by modified hydrophobic ZnO nanoparticle for membrane distillation, Asia-Pacific Journal of Chemical Engineering 13(3) (2018) e2196.

[8] L. Zeng, A method for preparing silica-containing iron(III) oxide adsorbents for arsenic removal, Water Research 37(18) (2003) 4351-4358.

[9] Y. Jeong, M. Fan, S. Singh, C.-L. Chuang, B. Saha, J. Hans van Leeuwen, Evaluation of iron oxide and aluminum oxide as potential arsenic(V) adsorbents, Chemical Engineering and Processing - Process Intensification 46(10) (2007) 1030-1039.

[10] L.N. Nthunya, L. Gutierrez, A.R. Verliefde, S.D. Mhlanga, Enhanced flux in direct contact membrane distillation using superhydrophobic PVDF nanofibre membranes embedded with organically modified SiO2 nanoparticles, Journal of Chemical Technology & Biotechnology 94(9) (2019) 2826-2837.

[11] F. Lan, J. Bai, H. Wang, The preparation of oleylamine modified micro-size sphere silver particles and its application in crystalline silicon solar cells, RSC Advances 8(30) (2018) 16866-16872.

[12] B.W. Chieng, N.A. Ibrahim, W.M.Z.W. Yunus, M.Z. Hussein, Poly(lactic acid)/Poly(ethylene glycol) Polymer Nanocomposites: Effects of Graphene Nanoplatelets, Polymers 6(1) (2014) 93-104.